Appl Phys A (2008) 93: 589–592
DOI 10.1007/s00339-008-4699-4

Applied Physics A
Materials Science & Processing

Impurity doping in silicon nanowires synthesized by laser ablation

N. Fukata · S. Matsushita · N. Okada · J. Chen · T. Sekiguchi · N. Uchida · K. Murakami

Received: 12 October 2007 / Accepted: 9 April 2008 / Published online: 13 June 2008

Abstract Boron (B) or phosphorus (P) doped silicon nanowires (SiNWs) were synthesized by laser ablation. Local vibrational modes of B were observed in B-doped SiNWs by micro-Raman scattering measurements at room temperature. Fano broadening due to a coupling between the discrete optical phonon and a continuum of interband hole excitations was also observed in the Si optical phonon peak for B-doped SiNWs. An electron spin resonance signal due to conduction electrons was observed only for P-doped SiNWs. These results prove that B and P atoms were doped in substitutional sites of the crystalline Si core of SiNWs during laser ablation and electrically activated in the sites.

PACS 81.07.Vb · 81.16.Mk · 63.22.+m · 65.80.+n · 78.30.Am

1 Introduction

One-dimensional silicon nanowires (SiNWs) are of great interest in the fields of both fundamental and application research. Until now, SiNWs have been synthesized by laser ablation [1–4] and chemical vapor deposition (CVD) [5, 6]. The advantage of the latter method is that the diameter of SiNWs can be controlled by the size of the metal catalyst particles which are placed on substrates in advance. This growth mechanism is called the vapor–liquid–solid (VLS) mechanism [7]. On the other hand, the advantage of the former method is that SiNWs can be synthesized in the gas phase without forming or placing metal catalysts of nanometer size as seeds for SiNWs. Not using nanometer-scale metal catalysts, however, makes it difficult to control the size and location of SiNWs. Recently, we investigated the synthesis parameters during laser ablation to realize the diameter control of SiNWs [8]. The result showed that the diameter can be controlled by the content of catalyst in ablation targets, synthesis temperature, and laser power. Furthermore, the laser ablation method makes it possible to synthesize a large number of SiNWs, leading to success in observing the phonon confinement effect, stress, and the states of dopant atoms in SiNWs [8–10].

In order to realize nanoscale silicon devices using SiNWs, it is important to investigate impurity doping. Recently, several results about boron (B) and phosphorus (P) doping in SiNWs have been reported [9–15]. In some of those reports [11–15], the doping effects have been investigated by electrical transport measurements.

In the present study, we performed B and P doping into SiNWs during laser ablation. The states of B atoms in SiNWs were investigated by micro-Raman scattering measurements at room temperature (RT), while those of P atoms in SiNWs were investigated by electron spin resonance (ESR) at 4.2 K.

N. Fukata (✉)
International Center for Materials Nanoarchitectonics, National Institute for Materials Science & PRESTO JST, Tsukuba 305-0044, Japan
e-mail: fukata.naoki@nims.go.jp

S. Matsushita · N. Okada · N. Uchida · K. Murakami
Institute of Applied Physics, University of Tsukuba, Tsukuba 305-8573, Japan

J. Chen · T. Sekiguchi
Advanced Electronic Materials Center, National Institute for Materials Science, Tsukuba 305-0044, Japan

2 Experiments

SiNWs were synthesized by laser ablation of a Si target with nickel as a metal catalyst and B and P as dopants, namely $Si_{89}Ni_1B_{10}$, $Si_{95}(Ni_2P)_5$, $Si_{98}(Ni_2P)_2$, and $Si_{99.5}(Ni_2P)_{0.5}$. For comparison, a $Si_{99}Ni_1$ target was used for the synthesis of undoped SiNWs. Furthermore, bulk-Si samples implanted with 50-keV $^{11}B^+$ ions at a dose of 5×10^{15} B^+ cm^{-2} or 1×10^{14} B^+cm^{-2} were also used to estimate the B concentration in SiNWs. The targets were placed in a quartz tube heated at 1200°C in flowing Ar gas. The growth of SiNWs is explained by the mechanism of VLS growth [7]. A frequency-doubled Nd:YAG laser (532 nm, 7-ns pulse width, 10 Hz, 150 mJ/pulse) was used to ablate the targets. SiNWs were directly deposited on a SiO_2 substrate for micro-Raman scattering measurements. SiNWs were also directly deposited on a Si substrate and then transferred to a quartz capsule for ESR measurements. Micro-Raman scattering measurements were performed at RT with a ×100 objective and 532-nm excitation light. The laser spot was about 1 μm. The excitation powers were set to be about 0.02 mW to avoid local heating effects due to the excitation laser [8]. ESR measurements were carried out at 4.2 K using an X-band ESR spectrometer with a magnetic field modulation of 100 kHz to investigate the state of P donors in SiNWs. A scanning electron microscope (SEM: JEOL, JSM-5610, 20 kV) and a scanning transmission electron microscope (STEM: Hitachi, S-5500, 30 kV) were used to observe the SiNWs and to investigate the details of their structures.

3 Results and discussion

Typical SEM and STEM images are shown in Fig. 1. The SEM image shows that a high density of SiNWs was synthesized by laser ablation. The STEM image shows that the SiNWs are composed of two layers. As we have already shown in our previous papers [4, 8], the core of the SiNWs is crystalline Si and the surface is amorphous SiO_x ($x < 2$). The diameter of the Si core is about 20 nm in Fig. 1b. The TEM measurements were also performed for B-doped SiNWs and P-doped SiNWs, showing that the doping did not affect the crystalline structure of SiNWs.

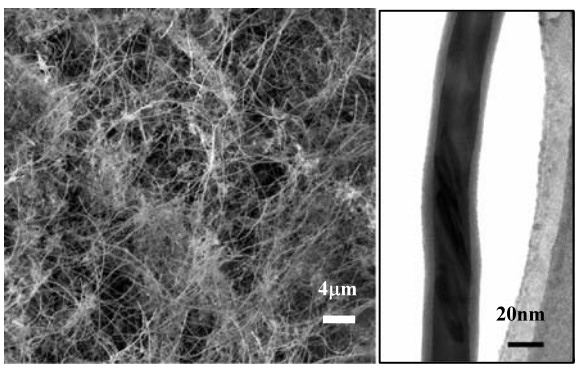

Fig. 1 Representative **a** SEM and **b** STEM images of the P-doped SiNWs

The results of micro-Raman scattering measurements for B-doped SiNWs, undoped SiNWs, and bulk Si are summarized in Fig. 2. The intense peak at about 520 cm^{-1} is attributed to the Si optical phonon peak. The optical phonon peak observed for B-doped SiNWs and undoped SiNWs showed a downshift compared to that for bulk Si. This is due to the phonon confinement effect [4, 16, 17]. Furthermore, the Si optical phonon peak for B-doped SiNWs is significantly broader than that for undoped SiNWs. This broadening can be explained by the Fano effect [18]. This result demonstrates heavy B doping into SiNWs during laser ablation since Fano broadening is due to coupling between discrete optical phonons and the continuum of interband hole excitations in degenerately doped p-type Si.

In Fig. 2b, Raman peaks were observed at about 618 and 643 cm^{-1}, in addition to the optical phonon peak at 520 cm^{-1}, for B-doped SiNWs. The peak frequencies are in good agreement with those of local vibrational modes of ^{11}B and ^{10}B in bulk Si crystal [19]. The intensity ratio of the two peaks in Fig. 2b reflects the natural abundances of ^{11}B (80.2%) and ^{10}B (19.8%); i.e. it is estimated as being roughly 4:1. Based on these results, the peaks at about 618 cm^{-1} and 640 cm^{-1} are surely attributed to the local vibrational modes of B in SiNWs. The observations of the Fano broadening and the B local vibrational peaks prove that

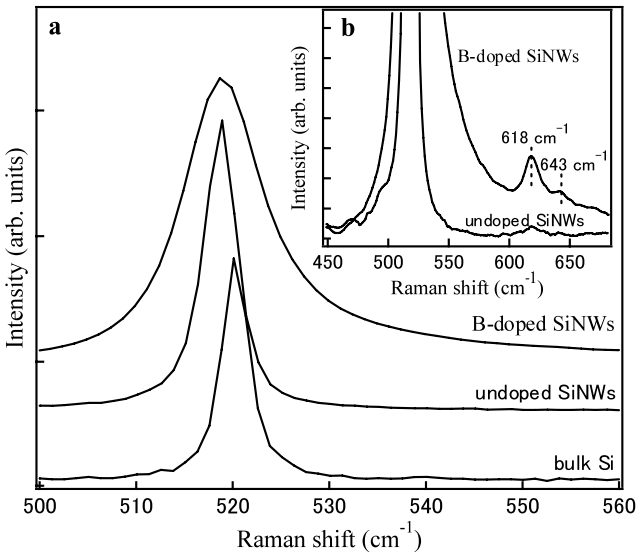

Fig. 2 **a** Optical phonon peaks of the SiNWs synthesized using a $Si_{89}Ni_1B_{10}$ target (B-doped SiNWs) and a $Si_{99}Ni_1$ target (undoped SiNWs) and that of bulk Si measured by micro-Raman scattering measurements. **b** Magnification of the Raman peak observed for B-doped SiNWs and undoped SiNWs

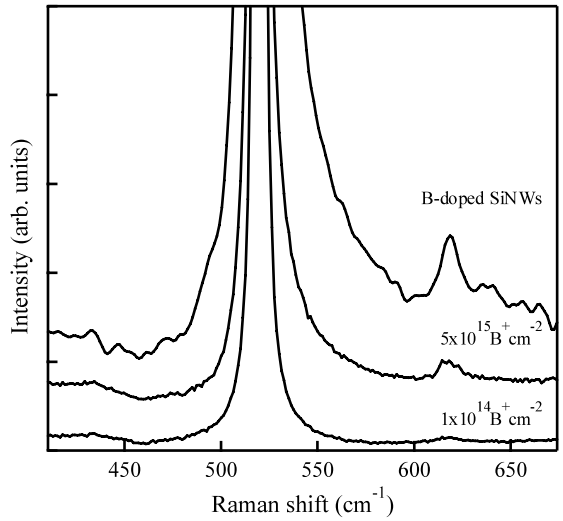

Fig. 3 Optical phonon peaks of the B-doped SiNWs and B-implanted bulk Si (50 keV, 5×10^{15} B^+ cm^{-2} and 1×10^{14} B^+ cm^{-2})

B atoms were electrically activated in substitutional sites of the crystalline Si core of SiNWs.

In the bulk Si, it is possible to estimate the electrically active B concentration by comparing the line-shape parameters deduced from the Raman spectra to those reported in the literature for different B concentrations [20]. In the case of SiNWs, however, asymmetric broadening due to the phonon confinement effect coexists in the Si optical phonon peak, making it difficult to obtain the line-shape parameters and finally the B concentration in B-doped SiNWs. In order to roughly estimate the B concentration in B-doped SiNWs, we performed Raman measurements for B-implanted bulk Si at the same conditions. The results are summarized in Fig. 3. The intensity of B local vibrational peaks and the Fano broadening for B-doped SiNWs were much larger than those for B-implanted bulk Si. This result indicates that the B concentration in the SiNWs is higher than that in B-implanted bulk Si. If B ions were implanted with a dose of 5×10^{15} cm^{-2}, the maximum concentration of B is in the order of 10^{19} cm^{-3}. Based on the results, the B concentration in SiNWs can be roughly estimated to be in a range exceeding 10^{19} cm^{-3}.

ESR measurements were performed at 4.2 K to investigate P donor/conduction electrons and defects in SiNWs as shown in Fig. 4a. The ESR signal was deconvoluted into three components with g-values of 1.998, 2.002, and 2.005. The ESR signal with the g-value of 1.998 was observed for P-doped SiNWs, but not observed for undoped SiNWs. The g-value is in good agreement with that of conduction electrons in bulk Si. Based on these results, the ESR signal with g-value of 1.998 is assigned to the ESR signal of conduction electrons, showing that P atoms were clearly doped in substitutional sites of the crystalline Si core of SiNWs and electrically activated in the sites. Several signals related to defects were also observed in the ESR signal for P-doped SiNWs. The ESR signal at 2.002 is due to defects in the surface oxide of SiNWs called *EX* centers [21]. The ESR signal at 2.005 is probably attributable to interfacial defects between the surface oxide and Si core of SiNWs, which are so-called P_b centers. We also observed a similar signal with g-value of 2.005 for nanocrystalline Si (nc-Si) embedded in SiO_2 [22]. P_b centers are well-known Si dangling bond centers ($Si_3{\equiv}Si\cdot$) formed at the Si/SiO_2 interface [23]. Three P_b variants have been observed: a defect called simply P_b at (111) Si/SiO_2 interfaces, and two defects called P_{b0} and P_{b1} at (100) Si/SiO_2 interfaces [24]. The precise g factors have been already obtained for (111) P_b ($g_{\parallel} = 2.0014$, $g_{\perp} = 2.0081$), (100) P_{b0} ($g_1 = 2.0087$, $g_2 = 2.0080$, $g_3 = 2.0015$), and (100) P_{b1} ($g_1 = 2.0076$, $g_2 = 2.0052$, $g_3 = 2.0012$). The g factors obtained for SiNWs and nc-Si are around 2.005, and the peak-to-peak line widths are broader than those previously reported [24–26]. Also, the line shapes are not Lorentzian but

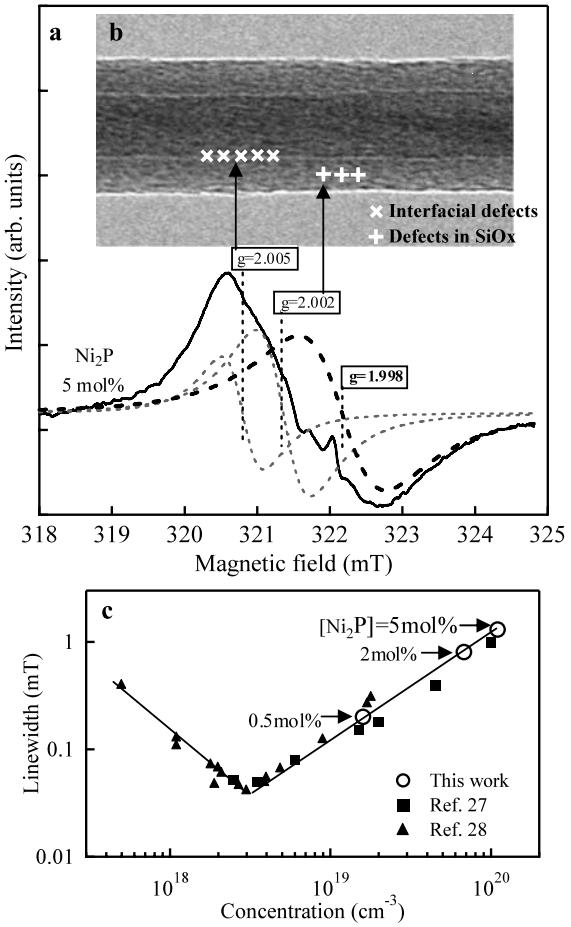

Fig. 4 **a** ESR spectra observed for undoped and P-doped SiNWs synthesized using $Si_{95}(Ni_2P)_5$ targets. The ESR signal for P-doped SiNWs was deconvoluted into three components. **b** A STEM image of SiNWs indicating defect species and locations. **c** Dependence of the ESR line width of conduction electrons on the P concentration

Gaussian. The surface geometries of the SiNWs and nc-Si are different from those of (111) Si/SiO_2 and (100) Si/SiO_2 interfaces, because the shapes of SiNWs and nc-Si are approximately cylindrical and spherical, respectively. Therefore, these have a range of crystallographic surfaces. These characteristic surface geometries cause slightly different g factors, resulting in broader line widths compared to the previously reported P_b centers and Gaussian line shapes.

In order to estimate the P concentration in P-doped SiNWs, we investigated the dependence of the ESR line width on P concentration. The ESR line width of P donor/conduction electrons significantly depends on the P concentration. The results of P-doped bulk Si [27, 28] are shown in Fig. 4c. We plotted the ESR line widths obtained for P-doped SiNWs under the assumption that the relationship obtained for bulk Si is true for the SiNWs. Based on the results of Fig. 4c, the P concentration in SiNWs can be roughly estimated to be in a range 10^{19}–10^{20} cm^{-3}. This result also suggests that the concentration of P donors is controllable by the content of P in the Si target.

4 Conclusion

We synthesized B- or P-doped SiNWs by laser ablation of Si targets with Ni as a metal catalyst and B and P as dopants. The local vibrational modes of B in SiNWs were observed for B-doped SiNWs. Fano broadening was also observed in the optical phonon peak for B-doped SiNWs, which indicates heavy B doping during laser ablation. These results prove that B atoms were doped in substitutional sites of the crystalline Si core of SiNWs during laser ablation and electrically activated in the sites. P doping in SiNWs during laser ablation was also confirmed by the ESR signal of conduction electrons. The concentration of P donors was controllable by the content of P in the Si target.

References

1. A.M. Morales, C.M. Lieber, Science **279**, 208 (1998)
2. Y.F. Zhang, Y.H. Tang, N. Wang, D.P. Yu, C.S. Lee, I. Bello, S.T. Lee, Appl. Phys. Lett. **72**, 1835 (1998)
3. S.T. Lee, N. Wang, C.S. Lee, Mater. Sci. Eng. A **286**, 16 (2000)
4. N. Fukata, T. Oshima, K. Murakami, T. Kizuka, T. Tsurui, S. Ito, Appl. Phys. Lett. **86**, 213112 (2005)
5. J. Westwater, D.P. Gosain, S. Usui, Jpn. J. Appl. Phys. **36**, 6204 (1997)
6. Y. Cui, L.J. Lauhon, M.S. Gudiksen, J. Wang, C.M. Lieber, Appl. Phys. Lett. **78**, 2214 (2001)
7. R.S. Wagner, W.C. Ellis, Appl. Phys. Lett. **4**, 89 (1964)
8. N. Fukata, T. Oshima, N. Okada, T. Kizuka, T. Tsurui, S. Ito, K. Murakami, J. Appl. Phys. **100**, 024311 (2006)
9. N. Fukata, J. Chen, T. Sekiguchi, N. Okada, K. Murakami, T. Tsurui, S. Ito, Appl. Phys. Lett. **89**, 203109 (2006)
10. N. Fukata, J. Chen, T. Sekiguchi, S. Matsushita, T. Oshima, N. Uchida, K. Murakami, T. Tsurui, S. Ito, Appl. Phys. Lett. **90**, 153117 (2007)
11. Y. Cui, X. Duan, J. Hu, C.M. Lieber, J. Phys. Chem. B **104**, 5213 (2000)
12. Y. Cui, C.M. Lieber, Science **291**, 851 (2001)
13. D.D.D. Ma, C.S. Lee, S.T. Lee, Appl. Phys. Lett. **79**, 2468 (2001)
14. K.K. Lew, L. Pan, T.E. Bogart, S.M. Dilts, E.C. Dickey, J.M. Redwing, Y. Wang, M. Cabassi, T.S. Mayer, S.W. Novak, Appl. Phys. Lett. **85**, 3101 (2004)
15. L. Pan, K.K. Lew, J.M. Redwing, E.C. Dickey, J. Cryst. Growth **277**, 428 (2005)
16. H. Richter, Z.P. Wang, L. Ley, Solid State Commun. **39**, 625 (1981)
17. I.H. Campbell, P.M. Fauchet, Solid State Commun. **58**, 739 (1986)
18. U. Fano, Phys. Rev. **124**, 1866 (1961)
19. C.P. Herrero, M. Stutzmann, Phys. Rev. B **38**, 12668 (1988)
20. M. Chandrasekhar, H.R. Chandrasekhar, M. Grimsditch, M. Cardona, Phys. Rev. B **22**, 4825 (1980)
21. A. Baumer, M. Stutzmann, M.S. Brandt, F.C.K. Au, S.T. Lee, Appl. Phys. Lett. **85**, 943 (2004)
22. N. Fukata, C. Li, H. Morihiro, K. Murakami, M. Mitome, Y. Bando, Appl. Phys. A **84**, 395 (2006)
23. Y. Nishi, Jpn. J. Appl. Phys. **10**, 52 (1971)
24. P.M. Lenahan, J.F. Conley Jr., J. Vac. Sci. Technol. B **16**, 2134 (1998)
25. L.G. Gosset, J.J. Ganem, H.J. von Bardeleben, S. Rigo, I. Trimaille, J.L. Cantin, T. Åkermark, I.C. Vickridge, J. Appl. Phys. **85**, 3661 (1999)
26. K.L. Brower, Phys. Rev. B **42**, 3444 (1990)
27. S. Maekawa, N. Kinoshita, J. Phys. Soc. Jpn. **20**, 1447 (1965)
28. J.D. Quirt, J.R. Marko, Phys. Rev. B **5**, 1716 (1972)